



Single-Cell Sequencing Reveals the Expression of Immune-Related Genes in Macrophages of Diabetic Kidney Disease

Xian Shao^{1,2}, Yueyue Shi³, Yao Wang⁴, Li Zhang^{1,2}, Pufei Bai^{1,2}, JunMei Wang^{1,2}, Ashanjiang Aniwang^{1,2}, Yao Lin^{1,2}, Saijun Zhou^{1,2} and Pei Yu^{1,2,5} 

Received 5 June 2023; accepted 13 September 2023

Abstract—Diabetic kidney disease (DKD) is characterized by macrophage infiltration, which requires further investigation. This study aims to identify immune-related genes (IRGs) in macrophage and explore their potential as therapeutic targets. This study analyzed isolated glomerular cells from three diabetic mice and three control mice. A total of 59 glomeruli from normal kidney samples and 66 from DKD samples were acquired from four kidney transcriptomic profiling datasets. Bioinformatics analysis was conducted using both single-cell RNA (scRNA) and bulk RNA sequencing data to investigate inflammatory responses in DKD. Additionally, the “AUCell” function was used to investigate statistically different gene sets. The significance of each interaction pair was determined by assigning a probability using “CellChat.” The study also analyzed the biological diagnostic importance of immune hub genes for DKD and validated the expression of these immune genes in mice models. The top 2000 highly variable genes (HVGs) were identified after data normalization. Subsequently, a total of eight clusters were identified. It is worth mentioning that macrophages showed the highest percentage increase among all cell types in the DKD group. Furthermore, the present study observed significant differences in gene sets related to inflammatory responses and complement pathways. The study also identified several receptor-ligand pairs and co-stimulatory interactions between endothelial cells and macrophages. Notably, SYK, ITGB2, FCER1G, and VAV1 were identified as immunological markers of DKD with promising predictive ability. This study identified distinct cell clusters and four marker genes. SYK, ITGB2, FCER1G, and VAV1 may be important roles. Consequently, the present study extends our understanding regarding IRGs in DKD and provides a foundation for future investigations into the underlying mechanisms.

KEY WORDS: diabetic kidney disease; single-cell RNA sequencing; marker genes; inflammation; macrophages.

Xian Shao, Yueyue Shi and Yao Wang contributed equally to this work and share first authorship.

¹NHC Key Laboratory of Hormones and Development, Chu Hsien-I Memorial Hospital and Tianjin Institute of Endocrinology, Tianjin Medical University, Tianjin 300134, China

²Tianjin Key Laboratory of Metabolic Diseases, Tianjin Medical University, Tianjin 300134, China

³Tianjin Medical University Cancer Institute and Hospital, Tianjin 300134, China

⁴Clinical Medical College & Affiliated Hospital of Chengdu University, Chengdu University, Chengdu, Sichuan 610081, People's Republic of China

⁵To whom correspondence should be addressed at NHC Key Laboratory of Hormones and Development, Chu Hsien-I Memorial Hospital and Tianjin Institute of Endocrinology, Tianjin Medical University, Tianjin, 300134, China. Email: peiyu@tmu.edu.cn

INTRODUCTION

According to the International Diabetes Federation, it is estimated that the diabetic population will reach 784 million by 2045, with a significant proportion (25–40%) developing diabetic kidney disease (DKD) during their lifetimes [1]. DKD is a significant public health concern as it is a major cause of impaired kidney function, proteinuria, and the need for renal replacement therapy [2]. The pathological characteristics of DKD include thickening of glomerular basement membrane, accumulation of mesangial matrix accumulation, and the presence of nodular glomerulosclerosis [3]. Despite the high prevalence of type 2 diabetes, renal biopsy is not routinely performed in most cases, leading to a lack of understanding regarding the underlying mechanisms of DKD.

Transcriptomic analysis of renal tissue or isolated glomeruli has provided insights into the pathogenesis of DKD and identified potential biomarkers [4]. However, previous studies on renal single-cell RNA sequencing (scRNA-seq) have primarily focused on cells from the proximal or collecting tubules, with a smaller proportion of glomerular cells captured, resulting in limited information on glomerular cells [5–7]. To overcome this limitation and obtain cell-specific gene expression information, Fu *et al.* performed scRNA-seq analysis on isolated glomerular cells from both DKD and control mice. Their findings revealed dynamic changes in gene expression within isolated glomerular cells, which may help identify crucial factors contributing to the progression of DKD [8].

Diabetic kidney injury is characterized by the infiltration of monocyte and macrophage [9]. The existence of distinct macrophage phenotypes in the kidney, along with their ability to transition between pro- and anti-inflammatory phenotypes, adds complexity to the development of therapeutic targets [10]. Macrophages accumulate in the diabetic kidney and are strongly associated with serum creatinine levels, accumulation of interstitial myofibroblast, and scores of interstitial fibrosis, thereby necessitating further exploration of the role of macrophages in DKD [11]. Fu *et al.* conducted a study on the transcriptome profiles of macrophages in early DKD, emphasizing their dynamic phenotype. However, the study lacked further analysis of immunologically relevant biomarkers that could be valuable for diagnosis [12].

Based on the scRNA-Seq data analysis of isolated glomerular cells, this study provides valuable insights into cell-specific processes, such as cell-cell interactions [8]. The research identified specific cell clusters and

inflammation-related genes (IRGs) associated with DKD, and further investigated glomerular cellular communication and potential therapeutic targets. Additionally, the study validated the expression patterns and potential regulatory mechanisms of IRGs in DKD using bulk RNA-seq data. The validation of the identified immune maker genes in mouse models emphasizes their potential contribution to the progression of DKD.

METHODS

Data Acquisition

ScRNA-seq data were obtained from the Gene Expression Omnibus (GEO) with GSE127235 as the accession number (<https://www.ncbi.nlm.nih.gov/geo/>). In this study, glomerular cells were isolated from three streptozotocin-induced diabetic endothelial nitric oxide synthase (eNOS)-deficient (eNOS^{-/-}) mice and three control eNOS^{-/-} mice [8]. This data was generated using the Illumina NextSeq 500 platform at the Genomics Core Facility. Additionally, four kidney transcriptomic profiling datasets were collected from GEO, including GSE96804, GSE104948, GSE30122, and GSE30528. The GSE96804 dataset (GPL17586 Affymetrix Human Transcriptome Array 2.0 platform) included 20 glomeruli from normal kidney samples and 41 glomeruli from DKD samples [13]. Additionally, the GSE104948 dataset consisted of 7 glomeruli from DKD samples (GPL22945 Affymetrix Human Genome U133 Plus 2.0 Array platform) [14]. The GSE30528 dataset had 13 glomeruli from normal kidneys and 9 from DKD samples, while the GSE30122 dataset included 26 glomeruli from normal kidneys and 9 from DKD samples (GPL571 Affymetrix Human Genome U133A 2.0 Array platform) [15].

Data Preprocessing

Principal component analysis (PCA) and uniform manifold approximation and projection (UMAP) analysis were performed using the Seurat R package (version 4.0.6). Cells with less than 50 genes or more than 7% mitochondrial genes were excluded from the analysis. A total of 1600 filtered cells were included in the analysis after applying quality control filters. The gene expression data was normalized and scaled using the

“LogNormalize” method provided by the Seurat package. Subsequently, the “vst” method was used to identify 2000 highly variable genes (HVGs) for each sample after data normalization.

Identify Marker Genes and Cell Clusters

To identify principal components (PCs), PCA was performed using the “RunPCA” function and 20 PCs were selected. Subsequently, the cells were then grouped into 8 different clusters with a resolution of 0.5 using the “FindNeighbors” and “FindClusters” functions. The UMAP were performed using the “RunUMAP” functions. For each cluster, “FindAllMarkers” was used to identify differentially expressed genes (DEGs) with a \log_2 fold-change (\log_2 FC absolute value) threshold of 0.5. The expression ratio of the cell cluster was set to ≥ 0.25 , and a significance level of $P < 0.05$ was used. To determine the cell type in each cluster, DEGs in each cluster were identified and manually checked using Cellmarker (<http://biocc.hrbmu.edu.cn/CellMarker/index.jsp>) and previous studies.

Bulk Sequencing Data Processing

Batch calibration was conducted on four datasets (GSE 96804, GSE104948, GSE30122, and GSE30528) using the “sva” R package (version 3.42.0). Differential gene analysis was performed using the “limma” R package. Genes with adjusted P values < 0.05 and \log_2 FC > 1 were identified as DEGs. The “ggplot2” R package (version 3.3.6) was used to generate the volcano and heat maps.

Protein-Protein Interaction Network (PPIs) Network Construction

The STRING website (<https://string-db.org/>) was used for the analysis of PPIs.

Weighted Gene Co-Expression Network Analysis (WGCNA)

By using the “WGCNA” function, the gene expression patterns were analyzed, and the association between modules and specific phenotypes was investigated.

Recognition of Key Transcription Factors

The Animal TFDB 2.0 (<http://bioinfo.life.hust.edu.cn/AnimalTFDB2/about.shtml>) was used to extract all identifiable transcription factors (TFs) associated with differential genes. To identify key transcription factors (TFs), we compared the list of TFs with the 97 significant differentially expressed genes (DEGs) obtained from both macrophage cluster and bulk RNA-seq data. The transcriptional regulatory networks of these key TFs were visualized with Cytoscape software (version 3.9.1).

GO and KEGG Analysis

The bulk RNA-seq data was analyzed using a bioinformatic tool (<https://www.xiantao.love/products>) to investigate the enriched Gene Ontology (GO) terms and Kyoto Encyclopedia of Genes and Genomes (KEGG) pathways. The selection of the top 10 pathways was based on the ranking of P values.

AUCell Scoring for IRGs and for Target Gene Sets

A total of 2483 immune genes were identified from the ImmPort database (<https://www.immport.org/shared/home>). Pathway scoring for individual cells was conducted using the “UCell” and “irGSEA” R packages (<https://chuiqin.github.io/irGSEA/index.html>). To estimate the proportion of highly expressed genes, gene expression rankings were calculated for each cell based on their expression profiles and the area under the curve (AUC) values of the IRGs. Cells with higher AUC values indicated a greater score of gene sets. Active cells were identified using an activity threshold. The “ggplot2” R package (Version 3.3.6) was used to visualize active clusters, with the AUC score for each cell being mapped to the UMAP. The expression of gene sets within each cell cluster was analyzed using the “irGSEA.heatmap” function. The upset graph displayed the number of gene sets with statistically significant differences for each cell cluster using the “irGSEA.upset” method. Furthermore, density scatter plots generated by the “irGSEA.density.scatterplot” function were used to illustrate the spatial expression levels of specific gene sets.

Cell-cell Communication Analysis

The analysis of cell-cell communication was performed using the CellChat R package (version 1.1.3). According to the CellChatDB database, the probabilities of secreted signaling, ECM-receptor, and cell-cell contact were obtained for different cell clusters. Overexpressed ligands or receptors within these clusters were identified. Subsequently, an interaction network was constructed using gene expression data. Ligand-receptor interaction pairs were identified whenever either the ligands or receptors was found to be overexpressed.

Immune Cell Infiltration Estimation

Transcriptome data was utilized to quantify the infiltration levels of 22 distinct immune cells types using the CIBERSORT deconvolution algorithm. The Wilcoxon test was used to compare the differences between the two groups, and the outcomes were visualized using the “vioplot” R package. Finally, the “Corrplot” R package was used to assess the association between immune cells.

Animal Models

The animal experiments were conducted in accordance with the protocols approved by the Animal Ethics Committee of Tianjin Medical University Chu Hsien-I Memorial Hospital (Tianjin, China). Male wild-type C57BL/6 mice were obtained from Huafukang Animal Centre (Beijing, China). The mice were kept in a pathogen-free facility at Chu Hsien-I Memorial Hospital.

In the WT-DM (wild-type diabetes mellitus) group, mice were fed an 8-week high-fat diet. Streptozotocin (Sigma-Aldrich, St. Louis, MO, USA) was intraperitoneally injected at a dosage of 60 mg/kg over a period of 5 days. WT-NC (wild-type negative control) groups received citrate buffer as a vehicle control. Diabetes was confirmed by fasting blood glucose (FBG) levels exceeding 16.7 mmol/L. Prior to euthanasia, 24-h urine and blood samples were collected to analyze the metabolic biochemical indices of the mice, including blood lipids, liver function, kidney function, and 24-h urine protein. The mice were euthanized at 12 weeks post-induction of DM. Kidney tissues were harvested from anesthetized mice and perfused with PBS before further processing.

Real-Time Quantitative Polymerase-Chain Reaction (RT-qPCR)

The total RNA from kidney tissue (0.10 g) was extracted using Trizol reagent (Solarbio, Beijing, China). Amplification of the target genes was performed using a SYBR green PCR kit (Toyobo, Japan) and an ABI Prism7300 fluorescent quantitative PCR instrument (ABI, USA). GAPDH was used as an internal control. The primer sequences of the target gene were as follows: VAV1: CGAACCTTCCTGTCTACTTGCTGTG (F), and CTCCTCTGCGGTGTCATCAATCTG (R); FCER1G: TCTCAGCCGTGATCTTGTCTTGC (F), and GGG TGGTTTCTCATGCTTCAGAGTC (R); ITGB2: TGT GCCGAGTGCCTGAAGTTTG (F), and ATGACCAGG AGGAGGACACCAATC (R); SYK: GAAGGCACA CCACTACACCATCG (F), and GACCGTCTGCTCTGA TTCATCTCTG (R).

The $2^{-\Delta\Delta C_t}$ method was used for semi-quantitative analysis of the mRNA expression of target genes.

Western Blot

Kidney tissues were added to RIPA lysate (Solarbio) and disrupted using ultrasound. After centrifugation (14,000 g; 4 °C; 15 min), the supernatant was collected. Protein extracts were quantified by a BCA assay and separated on 12% SDS denatured polyacrylamide gels. The separated proteins were transferred onto a NC membrane and blocking in 5% skim milk in TBST. Hybridization was performed using antibodies against rabbit SYK (1/2000; ab155187; Abcam), rabbit VAV1 (1/1000; A15108; ABclonal), rabbit ITGB2 (1/1000; A2173; ABclonal), rabbit FCER1G (1/1000; A12889; ABclonal), and mouse GAPDH (1/10000; AC033; ABclonal). GAPDH was used as the reference control. After incubation with a secondary antibody (1:3000–5000; zsbio), the protein was visualized using electrochemiluminescence (ECL).

Immunohistochemical Analyses

Immunohistochemical staining procedures were performed according to standard protocols on paraffin kidney sections. The kidney sections were subjected to incubation with primary antibodies, including rabbit SYK (1/200; ab155187; Abcam), rabbit VAV1 (1/100; A15108; ABclonal), rabbit ITGB2 (1/100; A2173; ABclonal), and rabbit FCER1G (1/100; A12889; ABclonal) at 4 °C

overnight. Subsequently, the sections were imaged using a light field microscope. To ensure unbiased selection, a blinded method was employed to randomly select three mice for each section.

Statistical Analyses

The statistical analysis was performed using R language (version 4.1.2) and Graphpad Prism software (version 8.0.1). Comparative analysis between groups was performed using Student's *t*-test. A *p*-value less than 0.05 was considered statistically significant, indicating a difference. To evaluate the predictive performance of the gene signature, time-dependent receiver operating characteristic (ROC) curves were generated using the "pROC" R package (version 1.18.0).

RESULTS

Single-Cell Transcriptome Analysis Reveals the Heterogeneity in Diabetes Kidney Disease

The graphic abstract shows the work flow of the study. The scRNA-seq data of three kidneys from mice with DKD and three controls mice were obtained from the GSE127235 dataset. After rigorous preprocessing, quality control, and normalization of the raw data, 800 cells from each group were retained. The nCount_RNA exhibited a positive correlation with nFeature_RNA, with a correlation coefficient of 0.66 (sFig. 1A, B). Subsequently, after normalizing the filtered scRNA-seq data, we selected the top 2000 HVGs. From these, we further identified the top 10 HVGs, which included MGP, CXCL13, IGHA, H2-Aa, CLIC3, H2-Ab1, IGKC, CCL2, CDKN1c, and KLK1 (sFig. 1C). The PCA analysis identified a total of twenty PCs with *P* values < 0.05 (sFig. 1D). Additionally, a total of eight clusters were identified, and for each cluster, the top 10 DEGs were listed (sFig. 1E).

The cells were divided into eight clusters using cluster analysis (Fig. 1a). These clusters were then assigned to known cell lineages using marker genes or DEGs (Fig. 1c). The cell types were identified by comparing the identified marker genes with published-type-specific markers. The identified cell clusters included tubular cells, endothelial cells, vascular endothelial cells, podocytes, mesangial cells, macrophages, proliferating cells, and B cells (Fig. 1a). The distribution of these clusters is shown in Fig. 1b, while the proportions of each cluster are depicted in Fig. 1d. In the context of DKD, the proportion

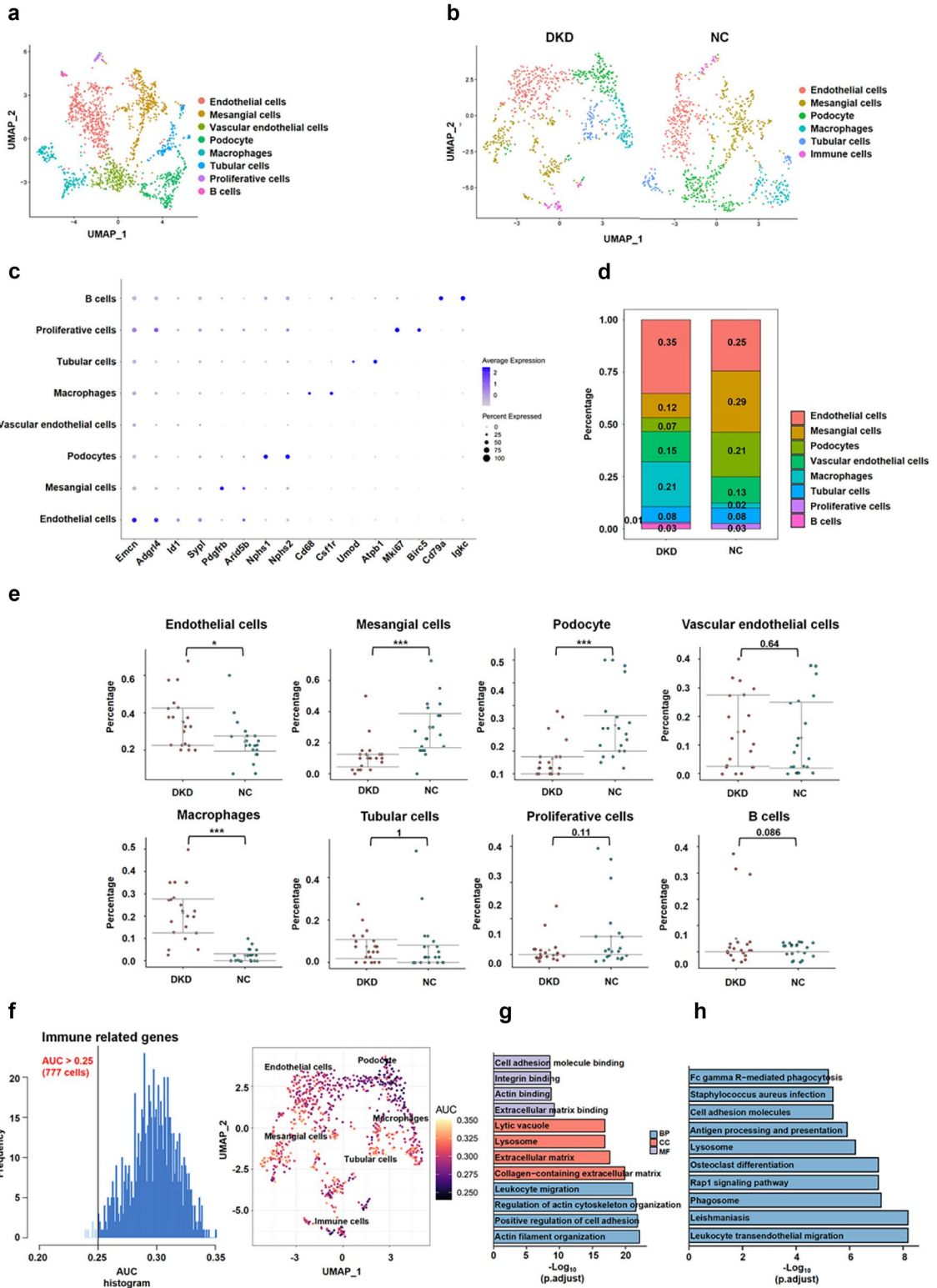
of macrophages was significantly higher compared to non-DKD (2% vs. 21%, *P* < 0.001), while mesangial cells (29% vs. 12%, *P* < 0.001), and podocytes (21% vs. 7%, *P* < 0.001) were significantly lower (Fig. 1e).

Macrophage sub-clusters were further identified using UMAP analysis, resulting in the identification of three clusters (sFig. 3A, B). Notably, the number of M2 macrophages was greater than that of M1 macrophages, and all sub-clusters of macrophages increased in the DKD group. DEGs in macrophage sub-clusters were subjected to GO and KEGG analysis. According to sFig. 3C, cluster 0 (M1 macrophages) exhibited up-regulated functions primarily associated with leukocyte adhesion and migration, cell proliferation, response to hypoxia, NIK/NF-kappaB, and Ras signaling pathway. Cluster 1 (M2 macrophages subtype I) showed mainly down-regulated functions, including phagocytosis, adhesion, apoptosis, and infection-related pathways. Cluster 2 (M2 macrophages subtype II) demonstrated higher activity compared to the other two clusters, with up-regulated functions related to tumor necrosis factor superfamily cytokine production and regulation, inflammatory response, migration, and adhesion.

AUCell Scoring of Cell Clusters in Diabetes Kidney Disease

According to the ImmPort database, a total of 2483 IRGs were obtained. The expression levels of IRGs within each cell cluster were assessed (Fig. 1f). Notably, macrophages, tubular cells, mesangial cells, and other immune cells in yellow coloration exhibited higher activity of IRGs. In macrophage clusters derived from DKD, DEGs were analyzed using the GO and KEGG databases. The identified terms were mainly associated with responses such as antigen processing and presentation, FcγR-mediated phagocytosis, and cell adhesion molecules (Fig. 1g, h).

We also utilized the "AUCell" function to examine if there were any significant differences in specific gene sets among cell clusters (Fig. 2a). Within the macrophage cluster, we observed a significant upregulation in several gene sets, including MYC targets V1, reactive oxygen species pathway, MYC targets V2, hypoxia cholesterol homeostasis, Mtorc1 signaling, E2F targets, PI3K AKT MTOR signaling, interferon gamma response, KRAS signaling UP, allograft rejection, TNFα signaling *via* NF-κB, inflammatory response, IL6/JAK/STAT3 signaling, and complement. To visually represent the



◀ **Fig. 1** Analysis of single-cell sequencing data in diabetic kidney disease. **a** Cell clusters were identified using UMAP analysis. Eight different cell types were assigned unique colors. **b** The UMAP projection of DKD and NC groups. **c** Dot plot of marker genes for each cell type clusters. Cell type identification was based on DEGs in each cluster and manually checked according to previous studies and the Cellmarker website. The intensity of color indicates average expression, while the size of dots represents percentage of cells expressing each gene. **d** The bar diagram shows the percentage of each cell cluster in DKD and NC groups. The numbers of cells in each cluster for DKD vs. NC are as follows: endothelial cells: 282 vs. 196; mesangial cells: 92 vs. 234; podocytes: 53 vs. 171; vascular endothelial cells: 116 vs. 100; macrophages: 171 vs. 19; tubular cells: 60 vs. 60; proliferative cells: 5 vs. 20; B cells: 20 vs. 0. **e** The dot diagram shows the percentage of each cell clusters in DKD and NC groups. The macrophage clusters show an increase in the DKD group. * means $P < 0.05$, ** means $P < 0.01$, and *** means $P < 0.001$. **f** IRG scores were calculated for cell clusters in DKD. The threshold is chosen as 0.25. The UMAP analysis displays the activity of IRGs in each cell cluster. Overall, macrophages express a higher number of IRG genes compared to other cell clusters. **g** The GO analysis was performed on DEGs in macrophage clusters from DKD. **h** The KEGG analysis was performed on DEGs in macrophage clusters from DKD. UMAP, uniform manifold approximation and projection; DKD, diabetic kidney disease; DEGs, differentially expressed genes; IRGs, immune-related genes; GO, Gene Ontology; KEGG, Kyoto Encyclopedia of Genes and Genomes; BP, biological process; CC, cell component; MF, molecular function.

distribution of significantly enriched gene sets within each cell cluster, we created a density scatter plot where a higher intensity of yellow color indicates a higher enrichment score (Fig. 2c). Additionally, we provided the number of gene sets that exhibited statistically significant differences within each cell cluster, as well as the intersections between them (Fig. 2b). Notably, podocytes displayed the highest number of differential gene sets.

Cell Communication Network Analysis in Diabetic Kidney Disease

To investigate the interactions among cell clusters, we utilized the “CellPhoneDB” function to identify receptor-ligand pairs. These pairs are essential for cellular communication, encompassing autocrine/paracrine signaling interactions, extracellular matrix (ECM) receptor interactions, and cell-cell contact interactions, which collectively play a key role in coordination of various biological processes. Using “CellChat,” we calculated the probability and significance of each interaction pair. The empirical shuffling method was used to ascertain the ligand-receptor pairs that exhibited significantly specificity toward certain cell types [16].

Through receptor-ligand interactions, immune cells closely interact with other cells (Fig. 3a, c, e). Autocrine/paracrine signaling interactions involved ligand-receptor pairs such as TGF β , IGF, CX3C, and complement signaling pathway network (Fig. 3b). Cell-cell interactions involved ligand-receptor pairs including LAIR1, CADM, ICAM, and ITGAL-ITGB2 signaling pathway network (Fig. 3d). Furthermore, ECM receptor interactions involved ligand-receptor pairs such as tenascin, THBS, collagen, and APP signaling pathway network (Fig. 3f).

Co-stimulatory interactions between endothelial cells and macrophages have been extensively observed, leading to the identification of specific ligand-receptor pairs such as CX3C, complement, and LAIR1. This finding implies that chemokines play a crucial role in the immune micro-environment and the regulation of macrophage infiltration in DKD. Additionally, the autocrine/paracrine signaling interaction network indicated the possibility of cross-talk among mesangial cells, endothelial cells, macrophages, and podocytes (Fig. 3a). It is worth noting that mesangial cells, endothelial cells, and macrophages have the potential to engage in cell-cell contact and ECM receptor interaction networks (Fig. 3c, e). Among the autocrine/paracrine signaling interactions, endothelial cells exhibit the highest degree of interaction with other cell types, followed by mesangial cells and macrophages.

Validation of Immune-Related Hub Genes and Immune Cell Infiltration Estimation in Bulk RNA Sequencing Data

To investigate the expression characteristics of glomeruli in patients with DKD, we conducted a comprehensive analysis by integrating data sets from GSE96804, GSE104948, GSE30122, and GSE30528. This analysis included a total of 66 DKD patients and 59 controls (Fig. 4a, b). We identified 46 up-regulated and 163 down-regulated DEGs (Fig. 4b). Furthermore, the top 10 terms of GO and KEGG showed a significant association with immune responses, which aligns with the findings obtained from scRNA-seq analysis.

We further investigated the common IRGs present in glomeruli cells and macrophage clusters in DKD. A total of 97 IRGs were identified (Fig. 4h). Among these, the expression of the top 35 common IRGs was mainly observed in macrophage clusters (Fig. 4j). Additionally, we examined the transcription factors (TFs) associated with the expression of DEGs. Notably, the highly active TFs in DKD included neurofibromatosis type 1 (NF1),

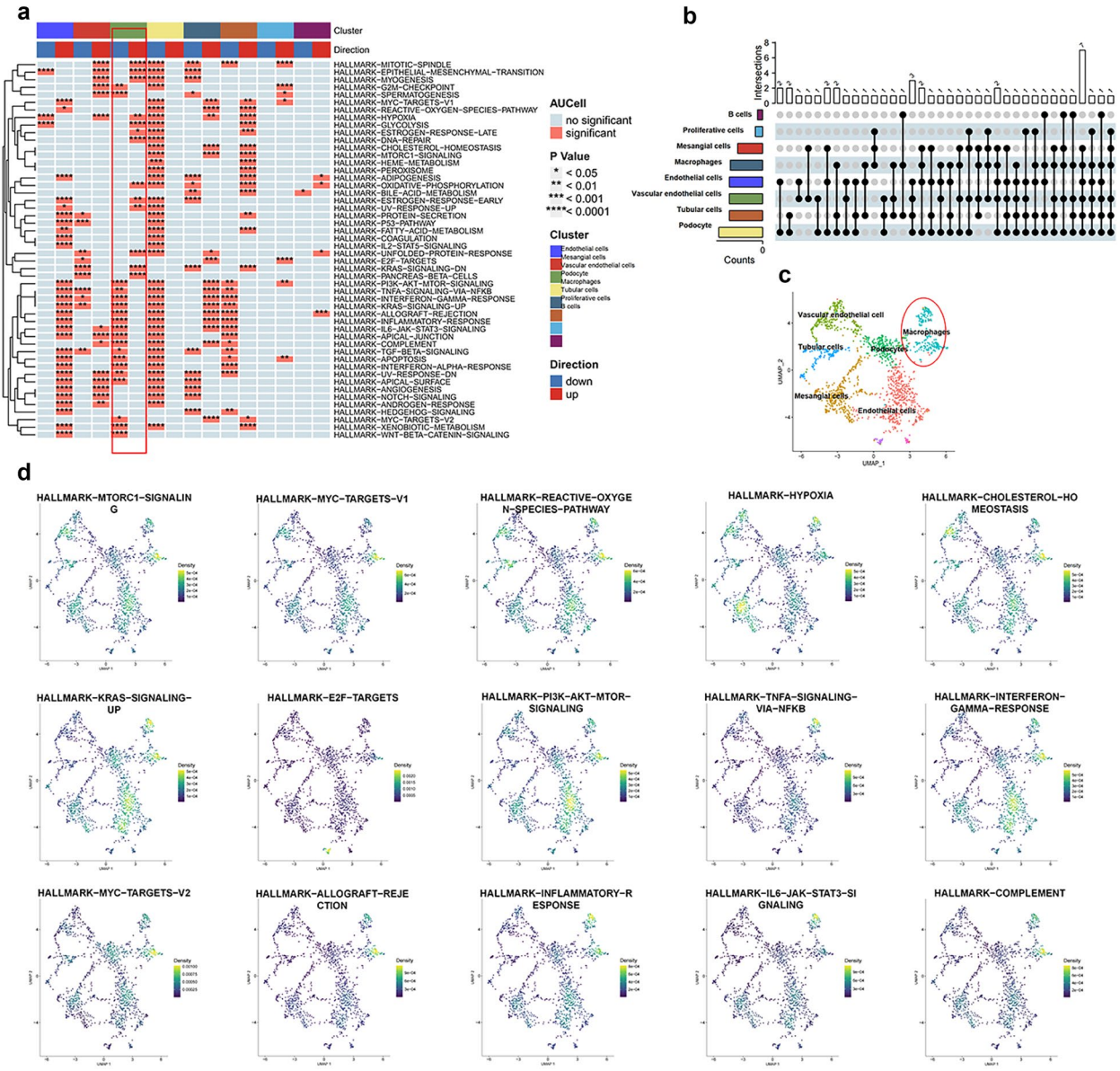


Fig. 2 Gene set enrichment analysis of all cell clusters. **a** Heatmap of gene set expression in all cell clusters. The heat map illustrates whether specific gene sets exhibit statistically significant differences in each cell clusters. Squares in blue indicate no statistical difference, while squares in red indicate a statistical difference. * means $P < 0.05$, ** means $P < 0.01$, *** means $P < 0.001$, and **** means $P < 0.0001$. The clustering tree on the left represents the similarity of expression patterns of different gene sets in cell clusters. The bars above represent the different cell clusters. The red bars indicate up-regulated differential gene sets, while blue bars represent down-regulated differential gene sets, respectively. **b** The number of significant enrichment pathways of cell clusters. The bars on the left represented the number of significant enrichment pathways in each cell clusters. The upper bar graph shows the number of cell clusters that gene sets were significantly enriched, while the bottom of graph represents the intersections between the cell clusters. **c** Cell clusters were identified using UMAP analysis. Eight different cell types were assigned unique colors. **d** Significantly enriched pathways in the macrophage cluster were displayed by UMAP analysis. These pathways include MYC targets V1, MYC targets V2, reactive oxygen species pathway, hypoxia cholesterol homeostasis, Mtorc1 signaling, E2F targets, PI3K/AKT/MTOR signaling, TNF- α signaling via NF- κ B, interferon gamma response, KRAS signaling UP, allograft rejection, inflammatory response, IL6 JAK STAT3 signaling, and complement.

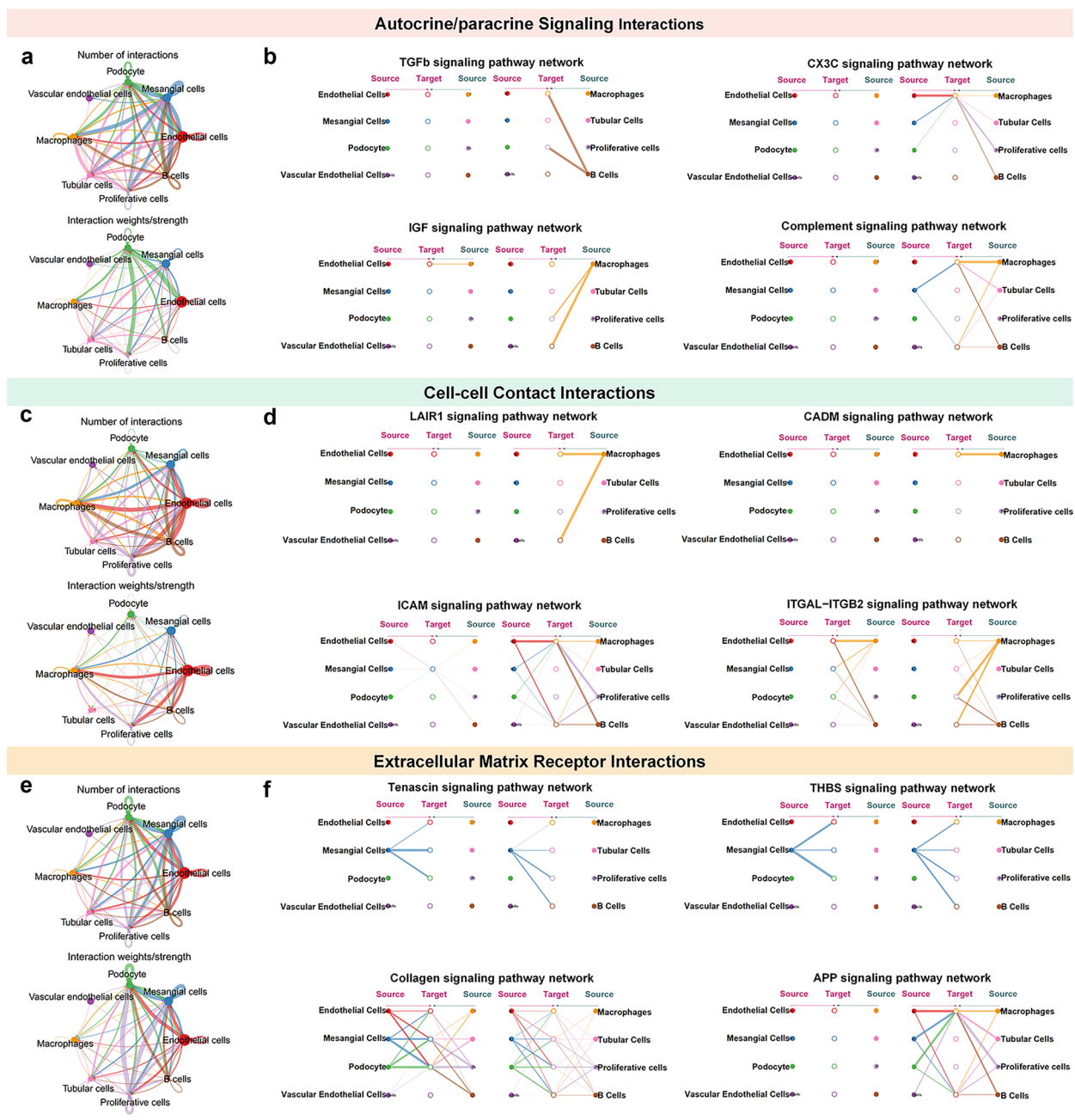


Fig. 3 Analysis of cell communication network in diabetes kidney disease. **a** The secreted signaling interaction network between cell clusters. The thickness of the connecting arm represents the number of interactions. **b** The common ligand-receptor pairs in autocrine/paracrine signaling interactions. The common ligand-receptor pairs involved in autocrine/paracrine signaling interactions include TGF-β, IGF, CX3C, and Complement signaling pathway network. **c** The cell-cell interaction network between cell clusters. The thickness of the connecting arm represents the number of interactions. **d** The common ligand-receptor pairs in cell-cell interactions. The common cell-cell interactions include tenascin, THBS, collagen, and APP signaling pathway network. **e** The extracellular matrix receptor interaction network between cell clusters. **f** The common ligand-receptor pairs in extracellular matrix receptor interactions. The common extracellular matrix receptors in secreted signaling are LAIR1, CADM, ICAM, and ITGAL-ITGB2 signaling pathway network.

nuclear factor kappa-B (NF- κ B), heat shock transcription factor 2 (HSF2), nuclear factor kappa-B p65 (NF- κ B65), P300, leukemia inhibitory factor (HLF), and TATA-box binding protein (TBP). Furthermore, Fig. 4i illustrates the highly up- and down-regulated genes ($|\logFC| > 1$).

The application of the WGCNA allowed for the identification of DEGs and their integration into distinct modules (sFig. 2A, B). A total of nine merged modules were successfully identified, with six of these modules demonstrating a significant association with DKD. Notably, the black module was predominantly associated with immune response, T cell activation, and leukocyte-mediated immunity.

To further elucidate the immune micro-environment in DKD, we conducted an analysis using the CIBERSORT classification to identify specific immune cell types infiltrating the glomerular tissue. Among the 22 immune cell types, our findings revealed significantly elevated levels of B cells ($P = 0.014$), dendritic cells ($P = 0.001$), resting state mast cells ($P = 0.004$), and M2 macrophages ($P < 0.001$) in DKD (Fig. 4c, g). Additionally, we explored the associations between infiltrating immune cells and observed a positive correlation between resting mast cells, memory B cells, dendritic cells, and M2 macrophages. Conversely, we observed a negative correlation between naive B cells, neutrophils, activated mast cells, and M2 macrophages (Fig. 4f).

Based on the analysis of the PPI network, it was observed that DEGs show strong interconnections (Fig. 5a). Hub genes, including SYK, LYN, ITGB2, FCER1G, VAV1, FGR, PIK3R1, HCK, PTK2, and LCP2, were identified due to their high number of nodes. To assess the diagnostic significance of these immune hub genes in relation to DKD, ROC curves were used (Fig. 5b). The results in Fig. 5b indicate that SYK, ITGB2, FCER1G, and VAV1 have AUC values of 0.777, 0.712, 0.703, and 0.742, respectively. This suggests that these four hub genes could serve as novel immunological markers for DKD, exhibiting favorable predictive capabilities.

Hub Gene Expression Validation in Diabetic Mouse Model

In the control group of mice, the kidneys exhibited a well-organized appearance, with intact glomeruli and normal tubules, as confirmed by H&E staining (Fig. 6a). On the other hand, the DT-DM group of mice showed signs of renal injury. Specifically, the proximal tubular lumen in the DT-DM group appeared enlarged, with

noticeable epithelial vacuolization, lighter cytoplasmic staining, tubular cell atrophy, and a reduction in tubular epithelial cells. Additionally, there was a decrease in the number of glomeruli, an increase in mesangial matrix, and thickening of the basement membrane (Fig. 6c).

Based on the qRT-PCR results, it was observed that the expression levels of SYK, ITGB2, FCER1G, and VAV1 were significantly higher in the kidney tissues of the WT-DM group compared to the WT-NC group (Fig. 6b). Immunohistochemical staining revealed higher expression levels of SYK, ITGB2, FCER1G, and VAV1 in the kidney tissues of the DM group when compared to the control group. Furthermore, Western blot analysis demonstrated a significant increase in the expression of SYK, ITGB2, FCER1G, and VAV1 proteins in kidney tissues from the DM groups.

DISCUSSION

In patients with diabetes, the presence of hyperglycemia and dyslipidemia activates the immune system. This activation triggers the release of inflammatory mediators by endothelial cells and podocytes, attracting monocytes/macrophages. This sets off an inflammatory cascade, leading to structural alterations in the kidneys and the development of tubulointerstitial fibrosis [17]. Inflammation plays a crucial role in the progression and onset of DKD, suggesting that targeting the immune system may be a more effective strategy than solely managing blood glucose levels or suppressing the renal-angiotensin system [18].

Macrophage infiltration in the glomeruli and interstitium of renal biopsies in DKD is a commonly observed phenomenon [19]. However, understanding of mechanisms by which macrophages migrate and home remains limited. Previous studies have indicated that renal parenchymal cells secrete monocyte chemoattractant protein-1 (MCP-1) and macrophage colony-stimulating factor 1 (M-CSF-1) to stimulate macrophage migration within the vascular endothelium and kidney [20, 21]. The continuous activation of inflammatory cytokines/chemokines, which aid in tissue repair, leads to excessive deposition of extracellular matrix and the development of renal fibrosis [19].

The functional characteristics of macrophages can significantly vary depending on the micro-environment [22]. Macrophages in the tissue micro-environment can be classified as either classically activated (M1) and

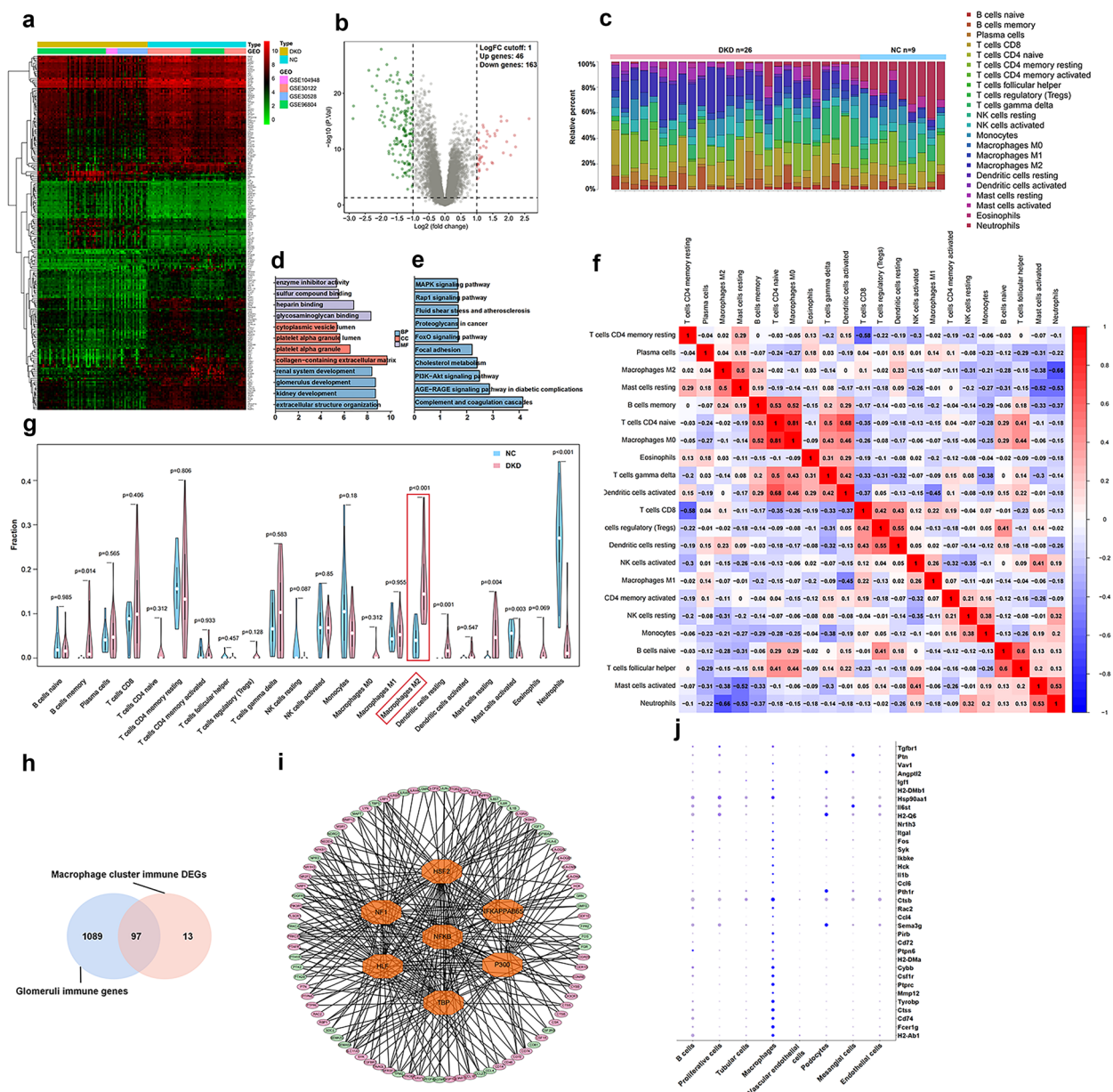


Fig. 4 Validation of immune-related hub genes and estimation of immune cell infiltration in bulk RNA sequencing data. **a** The heatmap of DEGs from 66 DKD patients and 59 controls. The dataset used for this analysis included GSE96804, GSE104948, GSE30122, and GSE30528. **b** The volcano plot of DEGs. Genes with an adjusted P value < 0.05 and $|\log_2(\text{fold change})| > 1$ were considered significant. Up-regulated genes represent in red, while down-regulated genes are shown in green. **c** Identification of specific immune cell types infiltrating in the glomerular tissue. **d** The top 10 terms from the GO analysis of DEGs. **e** The top 10 terms from the KEGG analysis of DEGs. **f** Association between infiltrating immune cells. **g** Proportion of macrophages marked by red boxes was significantly higher in the DKD group. **h** The Venn plot showing the common IRGs in DKD glomeruli cells and macrophage clusters. **i** Highly active TFs in DKD associated with the expression of common IRGs, including NF1, NF- κ B, HSF2, NF- κ B65, P300, HLF, and TBP. **j** Dot plot of expression of the top 35 common IRGs in the scRNA-seq dataset. The expression of these 35 IRGs was mainly active in macrophage clusters. DKD, diabetic kidney disease; DEGs, differentially expressed genes; IRGs, immune-related genes; GO, Gene Ontology; KEGG, Kyoto Encyclopedia of Genes and Genomes; TFs, transcription factors; NF1, neurofibromatosis type 1; NF- κ B, nuclear factor kappa-B; HSF2, heat shock transcription factor 2; NF- κ B65, nuclear factor kappa-B p65; HLF, leukemia inhibitory factor; TBP, TATA-box binding protein.

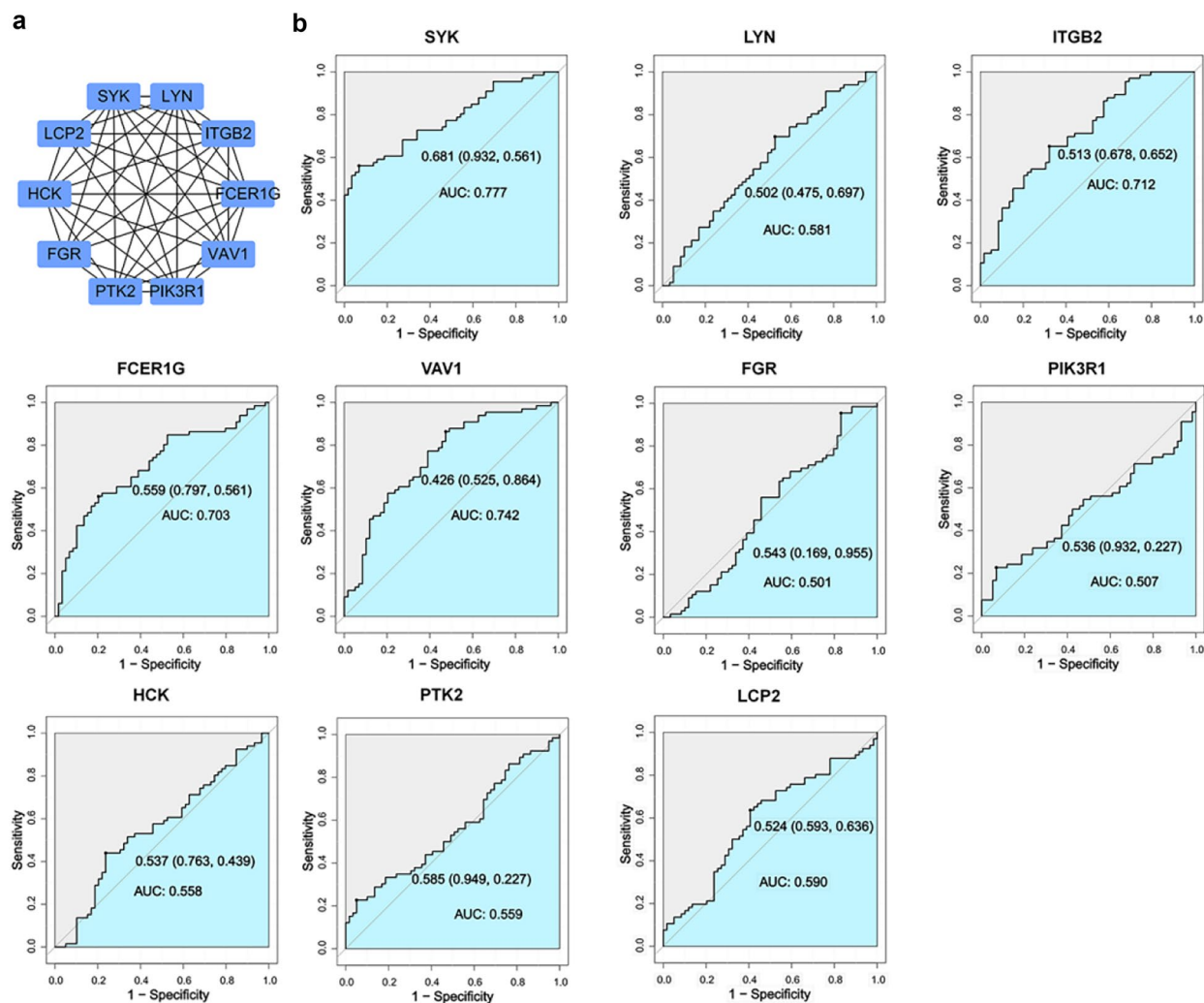


Fig. 5 The PPI network analysis identified hub gene from the DEGs. **a** The PPI network of DEGs. It revealed that SYK, LYN, ITGB2, FCER1G, VAV1, FGR, PIK3R1, HCK, PTK2, and LCP2 had the highest degree of connectivity and were identified as hub genes. **b** ROC curves were generated to assess the diagnostic potential of the hub genes for DKD. The AUC values of SYK, ITGB2, FCER1G, VAV1, LYN, PIK3R1, HCK, PTK2, and LCP2 are 0.777, 0.712, 0.703, 0.742, 0.581, 0.507, 0.558, 0.559, and 0.590, respectively. PPI, protein-protein interaction; DEGs, differentially expressed genes; ROC, receiver operating characteristic; DKD, diabetic kidney disease.

alternatively activated macrophages (M2) [23]. The accumulation of macrophages in the diabetic kidney is closely associated with the proliferation of interstitial myfibroblasts. However, the specific mechanisms by which subcluster of macrophages interact with the micro-environment remain unclear and require further investigation at the individual cell level. Therefore, the identification of effective approaches to prevent or treat fibrotic CKD poses a formidable challenge [24].

In this study, we successfully identified IRGs in DKD that could potentially be targeted for immunotherapy. To illustrate the immune cell composition and expression patterns of IRGs in glomerular tissue of DKD, we analyzed scRNA-seq data. Our analysis identified eight distinct clusters of cells, with a significantly higher proportion of macrophages observed in the DKD group compared to the control group. In order to gain deeper understanding of the immune micro-environment

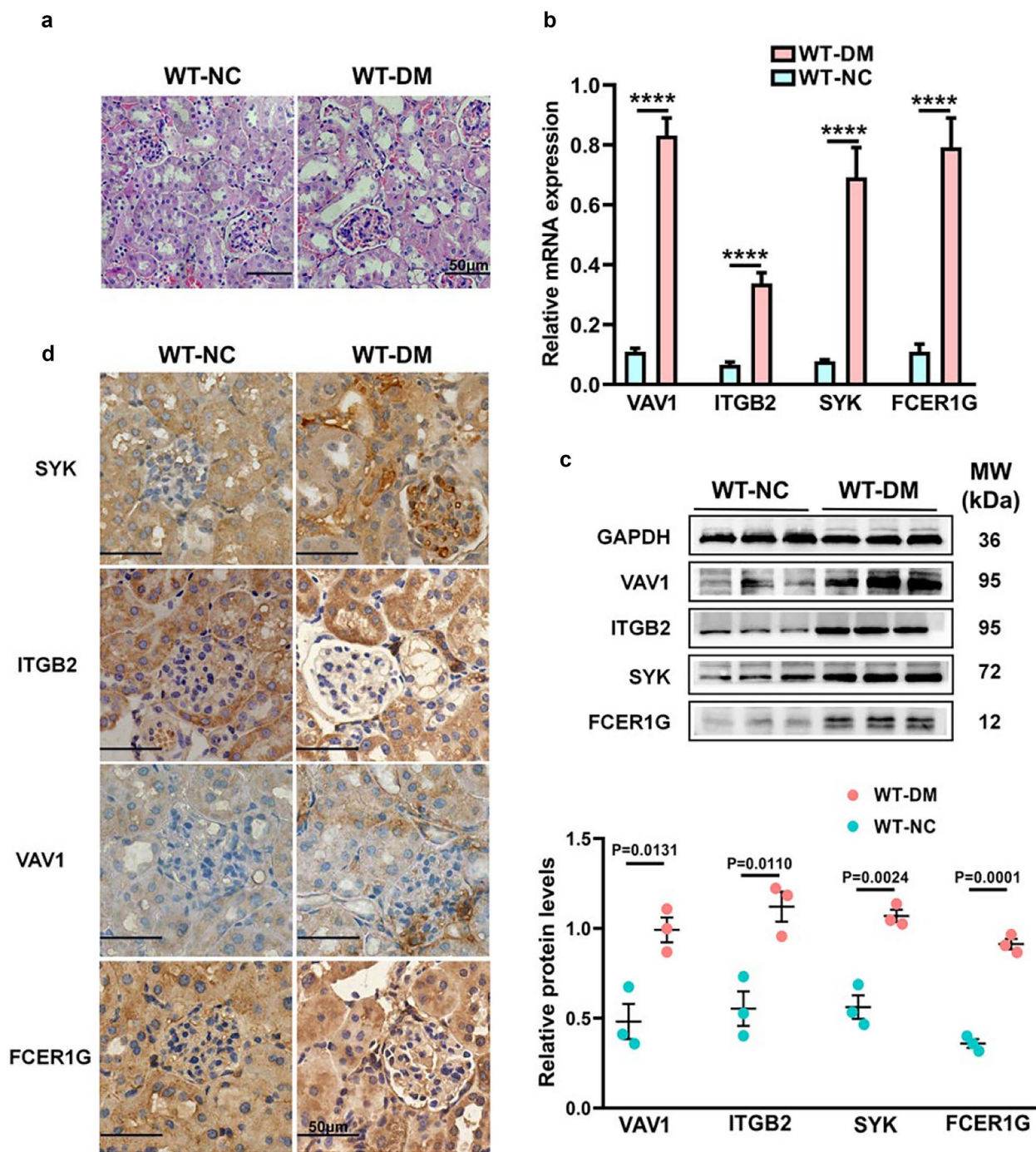


Fig. 6 Validation of hub gene expression in diabetic mouse model. **a** Kidney tissue samples from the WT-DM and WT-NC groups were stained with H&E. **b** mRNA expression levels of SYK, ITGB2, FCER1G, and VAV1 in kidney tissues from WT-DM and WT-NC group. **c** Protein expression levels of SYK, ITGB2, FCER1G, and VAV1 in kidney tissues from WT-DM and WT-NC groups. **d** Immunohistochemical staining was performed to assess the expression levels of SYK, ITGB2, FCER1G, and VAV1 in the kidney tissues.

in DKD, we verified our findings using bulk RNA-seq data to identify specific immune cell types that infiltrate the kidney. Our findings also indicated the presence and activation of macrophages in the renal tissue of DKD. Additionally, we calculated IRG scores, which revealed that cells with higher scores were predominantly macrophages, tubular cells, and other immune cells. Furthermore, we investigated whether specific gene sets exhibited significantly different across the identified cell clusters. There was a notable increase in the expression of gene sets related to inflammatory responses and complement pathways in macrophages. Additionally, the identification of receptor-ligand pairs and the widespread recognition of co-stimulatory interactions between endothelial cells and macrophages suggest that chemokines play a key role in regulating macrophage infiltration in the immune micro-environment of DKD.

A total of 46 up-regulated and 163 down-regulated DEGs were identified in the glomerulus-derived bulk RNA-seq data, using a cutoff value of adjusted $P < 0.05$ and $|\log\text{FC}| > 1$. The GO terms associated with the bulk RNA-seq data exhibited similarities to those observed in the scRNA-seq data. Furthermore, an investigation into the co-expression patterns of IRGs in DKD revealed that the expression of the first 35 common IRGs was notably active within macrophage clusters.

We have also identified a total of seven highly active TFs in DKD, namely, NF1, NF- κ B, HSF2, NF- κ B65, P300, HLF, and TBP. The receptor activator of NF- κ B and its ligands belong to the tumor necrosis factor and its receptor superfamily. Activation of NF- κ B facilitates the expression of immunoinflammatory factors and the recruitment of immune cell [17, 25, 26]. A previous study has demonstrated that downregulation of NF- κ B65 effectively prevented inflammation-induced kidney damage [27]. Additionally, the histone acetyltransferase p300 has been found to promote collagen activation and contribute to tubulointerstitial fibrosis in DKD [28]. However, further investigation is needed to determine the association between the other four TFs (NF1, HSF2, HLF, and TBP) and DKD. These TFs have the potential to significantly impact macrophage activation and localized kidney infiltration. Furthermore, the black module identified through WGCNA is predominantly associated with immune response and cytokine regulation.

By utilizing a PPI network and conducting ROC curve analysis, this study successfully identified several key genes (SYK, ITGB2, FCER1G, and VAV1) that have significant diagnostic predictive value for DKD. To

validate the expression of these genes, a mouse model of DKD was established. Through RT-qPCR, Western blot, and immunohistochemistry, it was confirmed that SYK, ITGB2, FCER1G, and VAV1 were significantly upregulated in diabetic mice. These findings not only enhance our understanding of the underlying molecular mechanisms of DKD but also provide potential therapeutic targets for the treatment of DKD.

Splenic tyrosine kinase (SYK) is a non-receptor cytoplasmic enzyme primarily expressed on mononuclear phagocytes (MNs) and B cells. It plays a crucial role in regulating inflammatory responses, maintaining immune homeostasis, and controlling macrophage and lymphocyte infiltration. Consequently, SYK serves as a significant immune signaling molecule and a potential therapeutic target [29]. Previous research has suggested that the SYK/JNK/NLRP3 signaling pathway may be involved in the pathogenesis of DKD [30]. Another study has demonstrated that SYK activates the TGF- β /Smad3 signaling pathway, while miR-136 inhibits renal tubular epithelial cell fibrosis by downregulation of SYK [31]. Additionally, SYK can activate the ERK and NF- κ B pathways and upregulate the transcription of TGF- β , thereby aggravating renal tubular injury [32]. Other studies have reported that high glucose prompts a swift activation of SYK, subsequently activating the NF- κ B pathway in glomerular cells. Conversely, the absence of SYK reversed this effect [33, 34]. As a result, SYK may play a role in chronic renal inflammation, tissue remodeling, and the progression of DKD.

While previous articles have confirmed the presence of VAV guanine nucleotide exchange factor 1 (VAV1) [35] and Fc epsilon receptor Ig (FCER1G) [36], additional validation is necessary to establish their role in the progression of DKD. Notably, FCER1G has been demonstrated to be a crucial gene implicated in cancer immune infiltration and micro-environment [37, 38]. In a study by Chun Chou *et al.*, it was observed that FCER1G-positive innate-like T cells exhibit significant cytotoxic potential, suggesting a potential new form of immune response induced by tumors [37]. VAV1, which acts as a guanine nucleotide exchange factor for Rho family guanosine triphosphatases, has been found to be essential for JNK activation [39]. Furthermore, VAV1 mutations have been implicated in the malignant transformation of T cells *in vivo* [40]. Additionally, VAV1 serves as a mediator for the transduction of the CD226 signaling pathway in macrophages [41]. Based on the expression of VAV1 and FCER1G and their involvement in innate immune signaling, it was hypothesized that these factors

could also impact chronic renal inflammation and tissue remodeling. However, the association between VAV1 and FCER1G and DKD remains poorly supported by evidence.

Several studies have identified ITGB2 as a potential biomarker for DKD [42–45]. However, there is currently a lack of experimental validation. Furthermore, ITGB2 has been demonstrated to contribute to the understanding of the relationship between CD8+ T cells and the key pathogenesis of diabetic retinopathy [46]. MRTF-A has also been implicated in the regulation of macrophage-endothelial cell adhesion in macrophages by activating ITGB2 transcription, and it is involved in the pathogenesis of myocardial hypertrophy [47]. Moreover, the integrin ITGAM-ITGB2/Mac-1 in macrophages plays a role in modulating LC3-associated phagocytosis [48]. In this study, we also identified the involvement of the signaling pathways of ICAM-1 and ITGAM-ITGB2 in cellular interactions that condition macrophage adhesion and phagocytosis. However, the available evidence regarding the function of ITGB2 in the macrophages of the local immune micro-environment in DKD and its regulation of phagocytosis remains limited.

There is growing evidence suggesting the involvement of the complement system in the progression of DKD [17]. Strong correlations have been observed between the levels of urinary complement activation products and renal tubular interstitial inflammation and injury [49]. Our study also identified a potential key role of the complement system; however, further elucidation through more precise study methods is needed.

This study employed bioinformatics technology to analyze immune-related biomarkers in macrophage clusters in DKD. By effectively identifying the most relevant gene for experimental validation, this approach reduces the time and cost associated with biological experiments. Consequently, this study enhances our understanding of the pathogenesis of macrophages in DKD and contributes to the development of potential therapeutic interventions. Ultimately, the findings of this study provide valuable guidance for the diagnosis and treatment of DKD. The present study has certain limitations. ScRNA-seq, although an advanced technique, is not exempted from shortcomings, such as sequencing coverage bias and low capture efficiency. Moreover, the data in this study were obtained from publicly available datasets, so any flaws in the study design were inherent to the original study. Therefore, it is essential to validate the current findings

through extensive *in vitro* and *in vivo* experiments and large cohorts to ensure reliable conclusions. Additionally, the sample size used in this study is relatively small. Future research endeavors should aim to increase the dataset by incorporating and analyzing a larger number of clinical samples to further validate these outcomes. Moreover, additional investigation is warranted to ascertain the potential correlation between the expression of immune-related hub genes and the severity of the disease.

CONCLUSION

In conclusion, this present study utilized scRNA-seq and bulk-seq data to conduct bioinformatics analysis, revealing the role of macrophages in kidney inflammation associated with DKD. These findings not only enhance our understanding of the significant contribution of macrophages to the progression of the DKD but also provide potential therapeutic targets for the treatment of DKD. Notably, macrophages showed the highest increase among all cell types in DKD tissues, suggesting their crucial role. Additionally, we successfully established a mice model of DKD and observed upregulation of macrophage-specific IRGs (SYK, ITGB2, FCER1G, and VAV1). These findings highlight the significance of macrophages and their marker genes as local immune factors in DKD. Overall, the present study expands our understanding of immune homeostasis in DKD and provides a foundation for future investigations into the underlying mechanisms.

SUPPLEMENTARY INFORMATION

The online version contains supplementary material available at <https://doi.org/10.1007/s10753-023-01906-2>.

AUTHOR CONTRIBUTION

Xian Shao: conceptualization, methodology, writing—original draft, investigation, validation, experiments, data curation, and visualization. Yueyue Shi and Yao Wang: conceptualization, validation, experiments, and review and editing. Li Zhang, Pufei Bai, JunMei Wang, Ashanjiang aniwang, and Yao Lin: validation, investigation, and experiments. Saijun Zhou: supervision and conceptualization. Pei Yu: conceptualization, resources, methodology, funding acquisition, supervision, and project administration. All authors reviewed and approved the manuscript.

FUNDING

This work was supported by financial support from Tianjin Science and Technology Major Special Project and Engineering Public Health Science and Technology Major Special Project (No. 21ZXGWSY00100), Tianjin Natural Science Foundation Key Project (No. 22JCZDJC00590), Tianjin Key Medical Discipline (Specialty) Construct Project (No. TJYXZDXK-032A), and Scientific Research Funding of Tianjin Medical University Chu Hsien-I Memorial Hospital (No. ZXY-ZDSYSZD-1).

DATA AVAILABILITY

All data generated and/or analyzed during the study are presented in this article and are available from the corresponding author upon reasonable request.

DECLARATIONS

Ethics Approval Animal experiments were performed with the approval of the Tianjin Medical University Animal Ethics Committee (No. 220916002).

Consent for Publication Written informed consent for publication was obtained from all participants.

Conflict of Interest The authors declare no competing interests.

REFERENCES

- de Boer, I.H., K. Khunti, T. Sadusky, et al. 2022. Diabetes management in chronic kidney disease: a consensus report by the American Diabetes Association (ADA) and Kidney Disease: Improving Global Outcomes (KDIGO). *Diabetes Care*. <https://doi.org/10.2337/dci22-0027>.
- Deng, Y., N. Li, Y. Wu, et al. 2021. Global, regional, and national burden of diabetes-related chronic kidney disease from 1990 to 2019. *Frontiers in Endocrinology* 12: 672350. <https://doi.org/10.3389/fendo.2021.672350>.
- Anders, H.J., T.B. Huber, B. Isermann, et al. 2018. CKD in diabetes: diabetic kidney disease versus nondiabetic kidney disease. *Nature Reviews. Nephrology* 14: 361–377. <https://doi.org/10.1038/s41581-018-0001-y>.
- Stewart, B.J., and M.R. Clatworthy. 2020. Applying single-cell technologies to clinical pathology: progress in nephropathology. *The Journal of Pathology* 250: 693–704. <https://doi.org/10.1002/path.5417>.
- Park, J., R. Shrestha, C. Qiu, et al. 2018. Single-cell transcriptomics of the mouse kidney reveals potential cellular targets of kidney disease. *Science* 360: 758–763. <https://doi.org/10.1126/science.aar2131>.
- Der, E., S. Ranabothu, H. Suryawanshi, et al. 2017. Single cell RNA sequencing to dissect the molecular heterogeneity in lupus nephritis. *JCI Insight* 2: e93009. <https://doi.org/10.1172/jci.insight.93009>.
- Wu, H., A.F. Malone, E.L. Donnelly, et al. 2018. Single-cell transcriptomics of a human kidney allograft biopsy specimen defines a diverse inflammatory response. *Journal of the American Society of Nephrology* 29: 2069–2080. <https://doi.org/10.1681/ASN.2018020125>.
- Fu, J., K.M. Akat, Z. Sun, et al. 2019. Single-cell RNA profiling of glomerular cells shows dynamic changes in experimental diabetic kidney disease. *Journal of the American Society of Nephrology* 30: 533–545. <https://doi.org/10.1681/asn.2018090896>.
- Perez-Morales, R.E., M.D. Del Pino, J.M. Valdivielso, et al. 2019. Inflammation in diabetic kidney disease. *Nephron* 143: 12–16. <https://doi.org/10.1159/000493278>.
- Katherine, R., R.A. Tuttle, Charles E. Alpers, George L. Bakris, Frank C. Brosius, Peter Kolkhof, and Jaime Uribarri. 2022. Molecular mechanisms and therapeutic targets for diabetic kidney disease. *Kidney International* 102: 248–260. <https://doi.org/10.1016/j.kint.2022.05.012>.
- Calle, P., and G. Hotter. 2020. Macrophage phenotype and fibrosis in diabetic nephropathy. *International Journal of Molecular Sciences* 21: 2806. <https://doi.org/10.3390/ijms21082806>.
- Fu, J., Z. Sun, X. Wang, et al. 2022. The single-cell landscape of kidney immune cells reveals transcriptional heterogeneity in early diabetic kidney disease. *Kidney International*. <https://doi.org/10.1016/j.kint.2022.08.026>.
- Pan, Y., S. Jiang, Q. Hou, et al. 2018. Dissection of glomerular transcriptional profile in patients with diabetic nephropathy: SRGAP2a protects podocyte structure and function. *Diabetes* 67: 717–730. <https://doi.org/10.2337/db17-0755>.
- Grayson, P.C., S. Eddy, J.N. Taroni, et al. 2018. Metabolic pathways and immunometabolism in rare kidney diseases. *Annals of the Rheumatic Diseases* 77: 1226–1233. <https://doi.org/10.1136/annrheumdis-2017-212935>.
- Woroniecka, K.I., A.S. Park, D. Mohtat, et al. 2011. Transcriptome analysis of human diabetic kidney disease. *Diabetes* 60: 2354–2369. <https://doi.org/10.2337/db10-1181>.
- Efremova, M., M. Vento-Tormo, S.A. Teichmann, et al. 2020. Cell PhoneDB: Inferring cell-cell communication from combined expression of multi-subunit ligand-receptor complexes. *Nature Protocols* 15: 1484–1506. <https://doi.org/10.1038/s41596-020-0292-x>.
- Tang, S.C.W., and W.H. Yiu. 2020. Innate immunity in diabetic kidney disease. *Nature Reviews Nephrology* 16: 206–222. <https://doi.org/10.1038/s41581-019-0234-4>.
- Chen, J., Q. Liu, J. He, et al. 2022. Immune responses in diabetic nephropathy: Pathogenic mechanisms and therapeutic target. *Frontiers in Immunology* 13: 958790. <https://doi.org/10.3389/fimmu.2022.958790>.
- Li, H.-D., Y.-K. You, B.-Y. Shao, et al. 2022. Roles and cross-talks of macrophages in diabetic nephropathy. *Frontiers in Immunology* 13: 1015142. <https://doi.org/10.3389/fimmu.2022.1015142>.
- Boels, M.G.S., A. Koudijs, M.C. Avramut, et al. 2017. Systemic monocyte chemotactic protein-1 inhibition modifies renal macrophages and restores glomerular endothelial glycocalyx and barrier function in diabetic nephropathy. *American Journal of Pathology* 187: 2430–2440. <https://doi.org/10.1016/j.ajpath.2017.07.020>.
- Lim, A.K., F.Y. Ma, D.J. Nikolic-Paterson, et al. 2009. Antibody blockade of c-fms suppresses the progression of inflammation and injury in early diabetic nephropathy in obese db/db mice. *Diabetologia* 52: 1669–1679. <https://doi.org/10.1007/s00125-009-1399-3>.

22. Park, M.D., A. Silvin, F. Ginhoux, et al. 2022. Macrophages in health and disease. *Cell* 185: 4259–4279. <https://doi.org/10.1016/j.cell.2022.10.007>.
23. Loke, P., and J.D. Lin. 2022. Redefining inflammatory macrophage phenotypes across stages and tissues by single-cell transcriptomics. *Science Immunology* 7: eabo4652. <https://doi.org/10.1126/sciimmunol.abo4652>.
24. Li, L., H. Fu, and Y. Liu. 2022. The fibrogenic niche in kidney fibrosis: components and mechanisms. *Nature Reviews. Nephrology* 18: 545–557. <https://doi.org/10.1038/s41581-022-00590-z>.
25. Wu, L., C. Liu, D.Y. Chang, et al. 2021. Annexin A1 alleviates kidney injury by promoting the resolution of inflammation in diabetic nephropathy. *Kidney International* 100: 107–121. <https://doi.org/10.1016/j.kint.2021.02.025>.
26. Ke, G., X. Chen, R. Liao, et al. 2021. Receptor activator of NF-kappaB mediates podocyte injury in diabetic nephropathy. *Kidney International* 100: 377–390. <https://doi.org/10.1016/j.kint.2021.04.036>.
27. Zhou, T., L. Sun, S. Yang, et al. 2020. 20(S)-ginsenoside Rg3 protects kidney from diabetic kidney disease via renal inflammation depression in diabetic rats. *Journal of Diabetes Research* 2020: 7152176. <https://doi.org/10.1155/2020/7152176>.
28. Xu, H., X. Wu, H. Qin, et al. 2015. Myocardin-related transcription factor A epigenetically regulates renal fibrosis in diabetic nephropathy. *Journal of the American Society of Nephrology* 26: 1648–1660. <https://doi.org/10.1681/ASN.2014070678>.
29. Wang, L., D. Aschenbrenner, Z. Zeng, et al. 2021. Gain-of-function variants in SYK cause immune dysregulation and systemic inflammation in humans and mice. *Nature Genetics* 53: 500–510. <https://doi.org/10.1038/s41588-021-00803-4>.
30. Qiao, Y., X. Tian, L. Men, et al. 2018. Spleen tyrosine kinase promotes NLR family pyrin domain containing 3 inflammasome-mediated IL-1beta secretion via c-Jun N-terminal kinase activation and cell apoptosis during diabetic nephropathy. *Molecular Medicine Reports* 18: 1995–2008. <https://doi.org/10.3892/mmr.2018.9164>.
31. Liu, L., X. Pang, W. Shang, et al. 2020. miR-136 improves renal fibrosis in diabetic rats by targeting down-regulation of tyrosine kinase SYK and inhibition of TGF-beta1/Smad3 signaling pathway. *Renal Failure* 42: 513–522. <https://doi.org/10.1080/0886022X.2020.1764854>.
32. Yang, W.S., J.W. Chang, N.J. Han, et al. 2012. Spleen tyrosine kinase mediates high glucose-induced transforming growth factor-beta1 up-regulation in proximal tubular epithelial cells. *Experimental Cell Research* 318: 1867–1876. <https://doi.org/10.1016/j.yexcr.2012.05.016>.
33. Yang, W.S., J.W. Seo, N.J. Han, et al. 2008. High glucose-induced NF-kappaB activation occurs via tyrosine phosphorylation of Ikap-paBalpha in human glomerular endothelial cells: involvement of Syk tyrosine kinase. *American Journal of Physiology. Renal Physiology* 294: F1065–F1075. <https://doi.org/10.1152/ajprenal.00381.2007>.
34. Yang, W.S., J.S. Kim, N.J. Han, et al. 2015. Toll-like receptor 4/ spleen tyrosine kinase complex in high glucose signal transduction of proximal tubular epithelial cells. *Cellular Physiology and Biochemistry* 35: 2309–2319. <https://doi.org/10.1159/000374034>.
35. Song, X., M. Gong, Y. Chen, et al. 2019. Nine hub genes as the potential indicator for the clinical outcome of diabetic nephropathy. *Journal of Cellular Physiology* 234: 1461–1468. <https://doi.org/10.1002/jcp.26958>.
36. Liu, S., C. Wang, H. Yang, et al. 2020. Weighted gene co-expression network analysis identifies FCER1G as a key gene associated with diabetic kidney disease. *Annals of Translational Medicine* 8: 1427. <https://doi.org/10.21037/atm-20-1087>.
37. Chou, C., X. Zhang, C. Krishna, et al. 2022. Programme of self-reactive innate-like T cell-mediated cancer immunity. *Nature* 605: 139–145. <https://doi.org/10.1038/s41586-022-04632-1>.
38. Morrish, E., and J. Ruland. 2022. Cytotoxic FCER1G(+) innate-like T cells: New potential for tumour immunotherapy. *Signal Transduction and Targeted Therapy* 7: 204. <https://doi.org/10.1038/s41392-022-01061-4>.
39. Huang, R., G. Guo, L. Lu, et al. 2019. The three members of the Vav family proteins form complexes that concur to foam cell formation and atherosclerosis. *Journal of Lipid Research* 60: 2006–2019. <https://doi.org/10.1194/jlr.M094771>.
40. Fukumoto, K., M. Sakata-Yanagimoto, M. Fujisawa, et al. 2020. VAV1 mutations contribute to development of T-cell neoplasms in mice. *Blood* 136: 3018–3032. <https://doi.org/10.1182/blood.2020006513>.
41. Ma, J., W. Hu, D. Zhang, et al. 2021. CD226 knockout alleviates high-fat diet induced obesity by suppressing proinflammatory macrophage phenotype. *Journal of Translational Medicine* 19: 477. <https://doi.org/10.1186/s12967-021-03150-4>.
42. Zhou, H., Z. Yang, L. Mu, et al. 2022. Integrated analysis of multiple microarray studies to identify core gene-expression signatures involved in tubulointerstitial injury in diabetic nephropathy. *BioMed Research International* 2022: 9554658. <https://doi.org/10.1155/2022/9554658>.
43. Xu, B., L. Wang, H. Zhan, et al. 2021. Investigation of the mechanism of complement system in diabetic nephropathy via bioinformatics analysis. *Journal of Diabetes Research* 2021: 5546199. <https://doi.org/10.1155/2021/5546199>.
44. Hu, Y., S. Liu, W. Liu, et al. 2021. Bioinformatics analysis of genes related to iron death in diabetic nephropathy through network and pathway levels based approaches. *PLoS One* 16: e0259436. <https://doi.org/10.1371/journal.pone.0259436>.
45. Geng, X.D., W.W. Wang, Z. Feng, et al. 2019. Identification of key genes and pathways in diabetic nephropathy by bioinformatics analysis. *Journal of Diabetes Investigation* 10: 972–984. <https://doi.org/10.1111/jdi.12986>.
46. Huang, J., and Q. Zhou. 2022. CD8+T cell-related gene biomarkers in macular edema of diabetic retinopathy. *Frontiers in Endocrinology* 13: 907396. <https://doi.org/10.3389/fendo.2022.907396>.
47. Liu, L., Q. Zhao, M. Kong, et al. 2022. Myocardin-related transcription factor A regulates integrin beta 2 transcription to promote macrophage infiltration and cardiac hypertrophy in mice. *Cardiovascular Research* 118: 844–858. <https://doi.org/10.1093/cvr/cvab110>.
48. Herb, M., A. Gluschko, and M. Schramm. 2018. LC3-associated phagocytosis initiated by integrin ITGAM-ITGB2/Mac-1 enhances immunity to *Listeria monocytogenes*. *Autophagy* 14: 1462–1464. <https://doi.org/10.1080/15548627.2018.1475816>.
49. Zheng, J.M., Z.H. Jiang, D.J. Chen, et al. 2019. Pathological significance of urinary complement activation in diabetic nephropathy: a full view from the development of the disease. *Journal of Diabetes Investigation* 10: 738–744. <https://doi.org/10.1111/jdi.12934>.

Publisher's Note Springer Nature remains neutral with regard to jurisdictional claims in published maps and institutional affiliations.

Springer Nature or its licensor (e.g. a society or other partner) holds exclusive rights to this article under a publishing agreement with the author(s) or other rightsholder(s); author self-archiving of the accepted manuscript version of this article is solely governed by the terms of such publishing agreement and applicable law.